Bioelectrochemistry 145 (2022) 108090

Contents lists available at ScienceDirect

Bioelectrochemistry

journal homepage: www.journals.elsevier.com/bioelectrochemistry

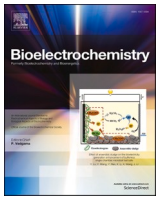

Electrochemical detection of caspase-3 based on a chemically modified M13 phage virus

Jae Hwan Shin [a], Anam Rana Gul [b], Moon Seop Hyun [c], Chang-Hyung Choi [d], Tae Jung Park [b,*], Jong Pil Park [a,*]

[a] Basic Research Laboratory, Department of Food Science and Technology, Chung-Ang University, Anseong 17546, Republic of Korea
[b] Department of Chemistry, Institute of Interdisciplinary Convergence Research, Research Institute of Chem-Bio Diagnostic Technology, Chung-Ang University, 84 Heukseok-ro, Dongjak-gu, Seoul 06974, Republic of Korea
[c] Department of Measurement & Analysis, National NanoFab Center (NNFC), 291 Daehangno, Daejeon 34141, Republic of Korea
[d] Division of Cosmetic Science and Technology, Daegu Haany University, 1 Haanydaero, Gyeongsan 38610, Republic of Korea

ARTICLE INFO

Keywords:
Caspase-3
Apoptosis
Electrochemical phage sensor
Chemical modification

ABSTRACT

Caspase-3, a cysteine-dependent protease, is considered a reliable molecular biomarker for the diagnosis and prognosis of apoptosis-related diseases. In this study, we demonstrated a phage-based electrochemical biosensor for the evaluation of cell apoptosis by the sensitive and specific detection of caspase-3. Specifically, for screening of affinity peptide-displayed phages, phage display was performed using M13 phage libraries (cyclic forms of peptides), and we identified potential affinity peptide-displayed phage clones with the sequence CPTTMWRYC. After characterization of its binding affinity using enzyme-linked immunosorbent assay, whole phage particles were covalently attached to a gold surface using coupling chemistry (MUA-EDC/NHS). The developed phage sensor was characterized by X-ray photoelectron spectroscopy (XPS), atomic force microscopy (AFM), scanning electron microscopy (SEM), electrochemical analysis using cyclic voltammetry (CV), and square wave voltammetry (SWV). Under optimal conditions, the affinity peptide-displayed phage sensor showed a good binding affinity ($K_d = 0.13 \pm 0.56$ μM) and limit of detection (0.39 μM) for caspase-3 detection. Furthermore, developed phage sensor could be monitored the response of apoptotic HeLa cells by detecting caspase-3 activity. This work should stimulate the development of efficient alternative caspase-3 detection methods for the diagnosis and prognosis of apoptosis-related diseases.

1. Introduction

Caspases are a family of cysteine proteases that play a central role in cell apoptosis which highly regulated and controlled cellular process for maintaining normal physiological metabolism and tissue homeostasis [1]. Thus, down regulation of apoptosis could play a role in many diseases, including cancers, neurological disorders, autoimmune diseases, and cardiovascular disorders [2,3,4]. Among the several types of caspases, caspase-3 is the most frequently activated protease in the apoptotic cell both by intrinsic and extrinsic pathways of apoptosis. Increased levels of caspase-3 can cause secretion of paracrine signaling factors that could promote cell proliferation in tumor cells [3,5,6]. Based on these factors, it is important to develop simple, sensitive, specific, and rapid methods for caspase-3 detection and further screening of potential inhibitors as apoptosis-related drugs [7].

Many analytical methods have been developed for the detection and quantification of caspase-3 activity, including colorimetric assays [8,9], fluorescence techniques [10,11], atomic force microscopy [12], surface-enhanced scattering [13], and surface plasma resonance [14]. Although these methods have admirable advantages, they can also be expensive, time-consuming, and labor-intensive. Alternatively, electrochemical detection methods are effective analytical techniques because of their simplicity, sensitivity, and rapid response [15,16].

Bioreceptors are a part of biosensors that can interact with target molecules, and mostly include antibodies, affinity peptides, aptamers, enzymes and cells [17,18,19,20,21,22]. Among the numerous bioreceptors, M13 phage is considerably resistant to harsh conditions caused by changes in pH, temperature, and protease activity [23]. Further, it is well-known that the M13 phage is harmless to the human system, and it could efficiently amplify in its host cells, and easily mass

* Corresponding authors.
E-mail addresses: tjpark@cau.ac.kr (T.J. Park), jppark@cau.ac.kr (J.P. Park).

https://doi.org/10.1016/j.bioelechem.2022.108090
Received 20 December 2021; Received in revised form 11 February 2022; Accepted 22 February 2022
Available online 24 February 2022

production with a high yield [24,25].

Herein, we aimed to develop an M13 phage-based electrochemical biosensor for the detection of caspase-3. First, the caspase-3-specific binding peptide-displayed phage was successfully identified by phage display and well-characterized using an enzyme-linked immunosorbent assay (ELISA). Then, whole phage particles were covalently attached to a gold surface using coupling chemistry (MUA-EDC/NHS), which is one of the most widely used methods. To the best of our knowledge, this is the first report on the fabrication of a whole M13 phage-based electrochemical biosensor capable of specific and sensitive detection of caspase-3.

2. Experimental section

2.1. Chemicals

Caspase-3 was obtained from Enzo Life Sciences (NY, USA), and bovine serum albumin (BSA) was obtained from Sigma-Aldrich (St. Louis, MO, USA). Thrombin and caspase-9, used for the control, were purchased from Roche (Basel, Switzerland) and Novus Biologicals (Centennial, USA), respectively. Caspase inhibitor (ZVADFMK) was purchased from Promega (Madison, USA). For the binding affinity tests, 2,2′-Azino-bis (3-ethylbenzothiazoline-6-sulfonic acid) diammonium salt (ABTS), horseradish peroxidase (HRP)-conjugated anti-M13 monoclonal antibody were purchased from Sino Biological (Beijing, China). For the coupling experiments, 11-mercaptoundecanoic acid (11-MUA), 1-ethyl-3-(3-dimethylaminopropyl) carbodiimide hydrochloride (EDC), N-hydroxy succinimide (NHS), potassium ferricyanide (III), potassium hexacyanoferrate (II) trihydrate, and ethanol were purchased from Sigma-Aldrich (St. Louis, MO, USA). For quantification of protein, bicinchoninic acid (BCA) assay kit was purchased from Pierce Biotechnology (MA, USA). RIPA lysis buffer and phenylmethylsulfonyl fluoride (PMSF) were purchased from Santa Cruz Biotechnology (Dallas, TX, USA). Dulbecco's Modified Eagle's medium (DMEM) was obtained from GenDepot (Katy, TX, USA), and fetal bovine serum (FBS) purchased from Thermo Fisher Scientific (Waltham, MA, USA). Unless otherwise stated, all chemicals were of analytical grade.

2.2. Escherichia coli strain and M13 phage

The *Escherichia coli* strain ER2738 and M13 peptide libraries (Ph.D.-C7C) were purchased from New England Biolabs. *E. coli* ER2738 was used as a host for infection of the M13 phage during whole process of biopanning.

2.3. Biotin labeling of caspase-3

For specific immobilization, caspase-3 was labeled with biotin using biotinylation kit (Thermo Scientific, USA). In biotin conjugation, 50 mM biotin was mixed with 100 μg of caspase-3 and incubated overnight on ice. Next, the mixtures were applied to Zeba desalting column to remove non-reacted biotin or residual reagents. Finally, the purified biotinylated protein concentration was measured using the BCA assay. The extent of biotin labeling on caspase-3 was determined using the 4′-hydroxyazobenzene-2-carboxylic acid (HABA)/avidin assay according the manufacturer's instructions.

2.4. Biopanning and DNA sequencing analysis

In the first round of biopanning, the biotinylated caspase-3 was separately pre-reacted with the Ph.D.-C7C random phage libraries ($\sim 10^{11}$ PFU/mL) at 100 rpm for 1 h at room temperature. After mild agitation of the phage-protein complexes, 100 μL of the complexes was introduced to the streptavidin-coated 96-well plates (Thermo Scientific) and allowed to react at 110 rpm for 10 min to facilitate specific binding between avidin and biotin. Then, 1 μL of biotin (0.1 mM) was added to competitively remove the phages which is non-specifically binding to the streptavidin-coated plate as a blocking agent and incubated for 5 min, followed by repeated washing 10 times using PBST buffer containing 0.1 M PBS with 0.1% Tween 20 for removing unbound phages and residual biotin. Finally, the bound phages were eluted in 0.2 M glycine-HCl (pH 2.2) with 1 mg/mL BSA solution. The eluent was neutralized with 15 μL of Tris-HCl (pH 9.0) to prevent deactivation or destruction of the desired phages. The eluted phages were amplified using *Escherichia coli* ER2738, and the amplified phage solution was quantified by phage titration for subsequent rounds of biopanning. During this biopanning, negative biopanning against streptavidin-coated plate was performed with the amplified phages in the beginning of the second round, and Tween 20 concentration of PBST was gradually increased (0.1–0.5%) for removing non-specifically binding phages.

Throughout successful biopanning, a total of four amplified M13 phages were analyzed using DNA sequencing. DNA sequencing analysis was performed by Solgent (Daejeon, Korea) as seen in Fig. S1, and yields were calculated for each round (Table S1).

2.5. ELISA assay

The relative binding affinities of the M13 phage candidates were measured using ELISA measurements as follows. First, the streptavidin-coated 96-well plates were pre-washed three times with 200 μL of 0.1 M PBS before protein immobilization, and the biotinylated caspase-3 was added to the functionalized streptavidin-coated plate and stirred at 110 rpm for 1 h. Subsequently, the unbound proteins were removed and then added blocking solution (5% BSA in $NaHCO_3$, pH 8.6) at 4 ℃ for 1.5 h. Then, the wells were washed six times with PBST buffer, and each phage were added at a concentration of 10^{12} PFU/mL, followed by stirring at 110 rpm at room temperature for 1 h. After washing six times with same buffer, horseradish peroxidase (HRP)-conjugated anti-M13 monoclonal antibody (1:2500 dilution in blocking buffer) was added and incubated for 1 h. The remaining solution was removed, and the plate was washed again with the same buffer. The ABTS and HRP substrate were added, and absorbance was measured at 405 nm (Multiskan, Thermo Scientific, Waltham, MA, USA).

2.6. Fabrication of phage sensor for detection of caspase-3

Preparation of a phage-based electrochemical biosensor was performed as follows (Scheme 1). First, the gold electrodes were cleaned sequentially with ethanol, distilled water, and piranha solution. The pretreated gold electrode was dried by blowing with N_2 gas, and then the gold electrode was reacted with 1 mM of MUA at room temperature for 14 h with mild shaking to introduce the thiol groups. Then, the gold electrode was incubated with EDC/NHS (800 mM:200 mM) at room temperature for 1 h. The carboxyl group of MUA and EDC were reacted to form the O-acylisourea intermediate, which then reacted with NHS to form NHS ester. After that, the gold electrode was further incubated with affinity peptide-displayed phage particles ($\sim 10^{12}$ PFU/mL) at room temperature for 1 h. Finally, the fabricated phage-based electrochemical biosensor was used for detection of caspase-3.

2.7. AFM, SEM and XPS analyses

Atomic force microscopy (AFM), scanning electron microscopy (SEM), and X-ray photoelectron spectroscopy (XPS) were used to examine the successful immobilization of the M13 phage onto the modified gold surface for development of electrochemical phage sensor. The AFM analysis was carried out using an XE-100 atomic force microscope (Park Systems, Korea) connected XEI offline software provided by Park Systems. The PointProbe® NCHR cantilevers (Nanoworld AG, Neuchâtel, Switzerland) were used for morphological imaging of the sample surface and all images were taken at the scan rate of 0.5 Hz under

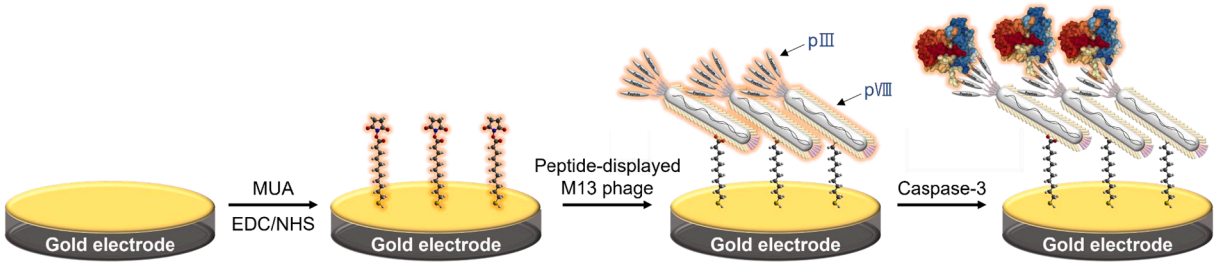

Scheme 1. Schematic illustration of the preparation of whole phage tethered gold surface and caspase-3 detection. The peptide-displayed phage was immobilized on the functionalized gold surface via coupling chemistry (MUA-EDC/NHS) which is able to react with the amine group in the N-terminal domain of the pVIII protein on the surface of M13 virion.

non-contact mode. The SEM measurements were performed using an SU8230 ultra-high-resolution field-emission scanning electron microscope (UHR-FE-SEM) (Hitachi, Japan). The SEM micrographs were obtained with a low energy accelerating voltage (1–5 kV) to reduce electron beam damage.

The XPS experiments were performed using K-Alpha + spectrometer (Thermo Scientific, USA). The high-resolution survey spectrum was recorded using Al K-Alpha X-ray source and a pass energy of 200 eV at a step size of 1.0 eV. XPS spectrums were taken with different gold surface conditions such as bare gold surface, MUA-treated gold surface, MUA-EDC/NHS-treated gold surface, and whole phage-tethered gold surface. AFM and SEM investigations were taken at the bare gold surface and whole phage-tethered gold surface.

2.8. Electrochemical measurements using CV and SWV

All electrochemical measurements were performed using the conventional three-electrode system, including a gold working electrode (diameter: 5 mm, surface area: 19.6 mm^2), platinum counter electrode, and Ag/AgCl reference electrode in 2.5 mM ferro/ferricyanide as an electron mediator in 1 M KNO_3. Cyclic voltammetry (CV) and square wave voltammetry (SWV) were performed on CHI 660E (CH Instruments Inc., USA). CV measurements were conducted in the range of −1 to 1 -V with a step potential, amplitude, and frequency of 4, 5, and 10 Hz, respectively. SWV measurements were conducted in the range of −400 to 800 mV with a step potential, amplitude, and frequency of 5 mV and 10 Hz, respectively. The relative current change (ΔI %) in SWV was determined by the following relationship based on the decreased peak current obtained after immobilization of M13 phages and caspase-3 interaction using the following equation:

$\Delta I\ \% = (I_0\text{-}I)/I_0 \times 100$, where I_o refers to gold-phage oxidation current before the addition of protein and I to the gold-protein oxidation current.

2.9. HeLa cell culture for caspase-3 assay

HeLa cells were purchased from American Type Culture Collection (ATCC) and cultured in Dulbecco's Modified Eagle's medium (DMEM) containing 10% fetal bovine serum (FBS) and 1% antibiotics at 37 °C under a humidified atmosphere of 95% air and 5% CO_2. For assay of caspase-3, HeLa cells were seeded with 4×10^3 cells per well onto a cover glass-bottom dish (100 mm × 20 mm, SPL, Pocheon, Korea) and then incubated for 24 h. After that, cells culture media was replaced with different doxorubicin (DOX) concentration in a range of 5–20 μM and incubated at different time intervals (6, 12, 24, and 48 h) at 37 °C under a humidified atmosphere of 5% CO_2. After incubation, HeLa cells were removed from the culture dish with a cell scraper and transferred the resulting lysate to a microcentrifuge tube. The adherent cells were then washed three times by low-speed centrifugation (200*g*, 5 min, 4 °C) with fresh and ice-cold phosphate-buffered saline (PBS buffer, pH 7.4) to remove culture medium and rinse cell monolayer. 0.6 mL of RIPA lysis buffer mixed with protease inhibitors was added and gently rocked for 30 min at 4 °C. Subsequently, 10 μL of PMSF (10 mg/mL) was added, and the first lysate was incubated for 60 min on ice. The whole cell lysate was centrifugated at 10,000*g* for 10 min at 4 °C. The supernatant fluid was transferred to a new microtube and used directly for caspase-3 assay without further purification.

3. Results and discussion

3.1. Identification of potential affinity peptide-displayed phage for caspase-3

The biopanning with random peptide libraries (Ph.D.-C7C) were performed to identify the M13 phage capable of specific binding to caspase-3. It is noted that C7C library in which a peptide could form a cyclic or ring structure through disulfide bonding between one of its cysteine residues and the cysteine on the end of pIII protein of M13 phage to screen for an affinity peptide, like 'CXXXXXXXC' structure (X is random amino acid). During the four rounds of biopanning, the yield gradually increased from the first to the fourth round (Table S1). In this process, the selection was anchored in the most commonly occurring peptides in each round. Interestingly, we also observed that each peptide has same binding motif, like neutral residues (e.g. threonine and tyrosine), basic residues (e.g. arginine and lysine), and hydrophobic residues (e.g. threonine and tyrosine), indicating that electrostatic interactions, hydrophobic interactions and/or hydrogen bonds are probably concerned in the binding of caspase-3. Based upon these standards, four phage clones were chosen to compare their binding affinities. These identified peptide sequences are shown in Table S2, and their binding affinities for caspase-3 were tested by ELISA (Fig. 1). For these experiments, 0.05 μM of caspase-3 or the same concentration of BSA, as a non-specific binding control, was immobilized on a streptavidin-coated plate, and 10^{12} PFU/mL of phages were added to each plate. Finally, we observed that C7C 2-18 phages had a higher affinity than the other candidates, as shown in Fig. 1A. From these observations, we chose C7C 2-18 phages for further characterization. Next, we tested the binding affinities of C7C 2-18 phages at different phage concentrations. The results showed that binding affinity of C7C 2-18 phages increased with increasing phage concentration within a range of 10^8–10^{12} PFU/mL (Fig. 1B). This may possible due to the avidity effects because there are usually 3–5 copies of peptides per phage and the change of ELISA signal is proportional to amount of bound caspase-3 which is indicative relative binding affinities of peptides. Subsequently, we observed the relative binding affinities C7C 2-18 phages at different caspase-3 concentrations (Fig. 1C). As increasing caspase-3 concentration, the signal of absorbance was also increased. The results of these experiments indicated that C7C 2-18 could be used as a phage virus-based receptor for highly selective and specific detection of caspase-3.

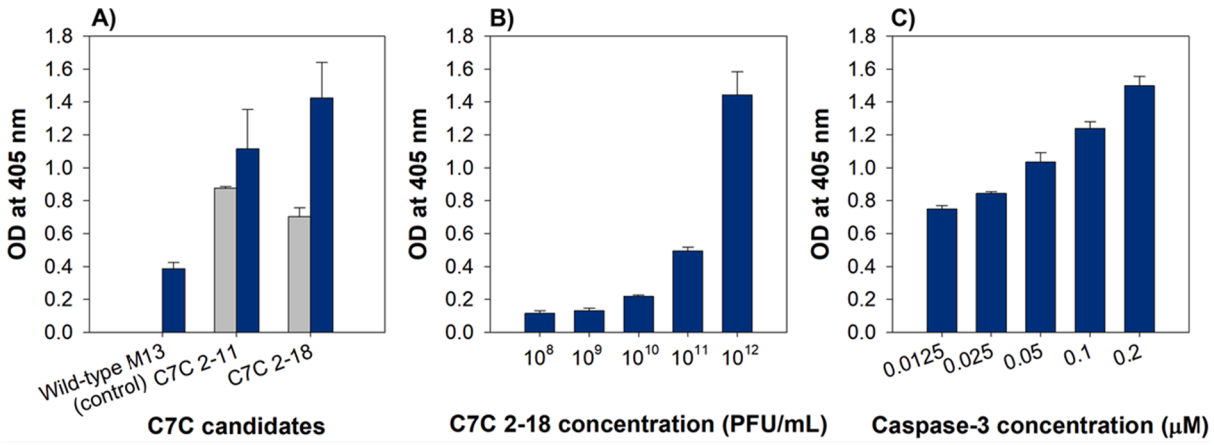

Fig. 1. Characterization of the selected phages using ELISA. (A) Selection of caspase-3 specific binding phage. (B) Effect of phage concentration. (C) Effect of protein concentration. The gray bar indicates BSA (negative control) and the blue bar indicates caspase-3. All measurements were done in triplicate, and error bars represent standard deviations.

3.2. Development of phage-based biosensor

3.2.1. Optimization of chemical modification and electrochemical behavior of modified gold electrodes

As a reproducible, stable, and well-established receptor production method, chemical modification on a gold surface was implemented to chemically immobilize the M13 phage. To achieve this purpose, we used MUA-EDC/NHS coupling chemistry for specific immobilization of whole phages on the gold surface. The electrochemical behavior of the bare gold electrode, MUA-treated gold electrode, MUA-EDC/NHS-treated gold electrode, and whole phage-tethered gold surface was examined using CV, which demonstrated an apparent redox peak ascribed to Fe $(CN_6)^{3-/4-}$ for each modified electrode (Fig. 2A). We observed that the peak currents from the Fe$(CN_6)^{3-/4-}$ redox decreased when immobilized 11-MUA on the gold surface. This could be ascribed to the fact that the 11-MUA with a long $-CH_2$ backbone and $-COO^-$ groups hindered the diffusion of Fe$(CN_6)^{3-/4-}$ because of its hydrophobic properties and electrostatic repulsion. After $-COO^-$ residues at the terminal of 11-MUA were replaced by NHS ester through the EDC/NHS reaction, electrostatic repulsion was partially eliminated and thus the redox currents were

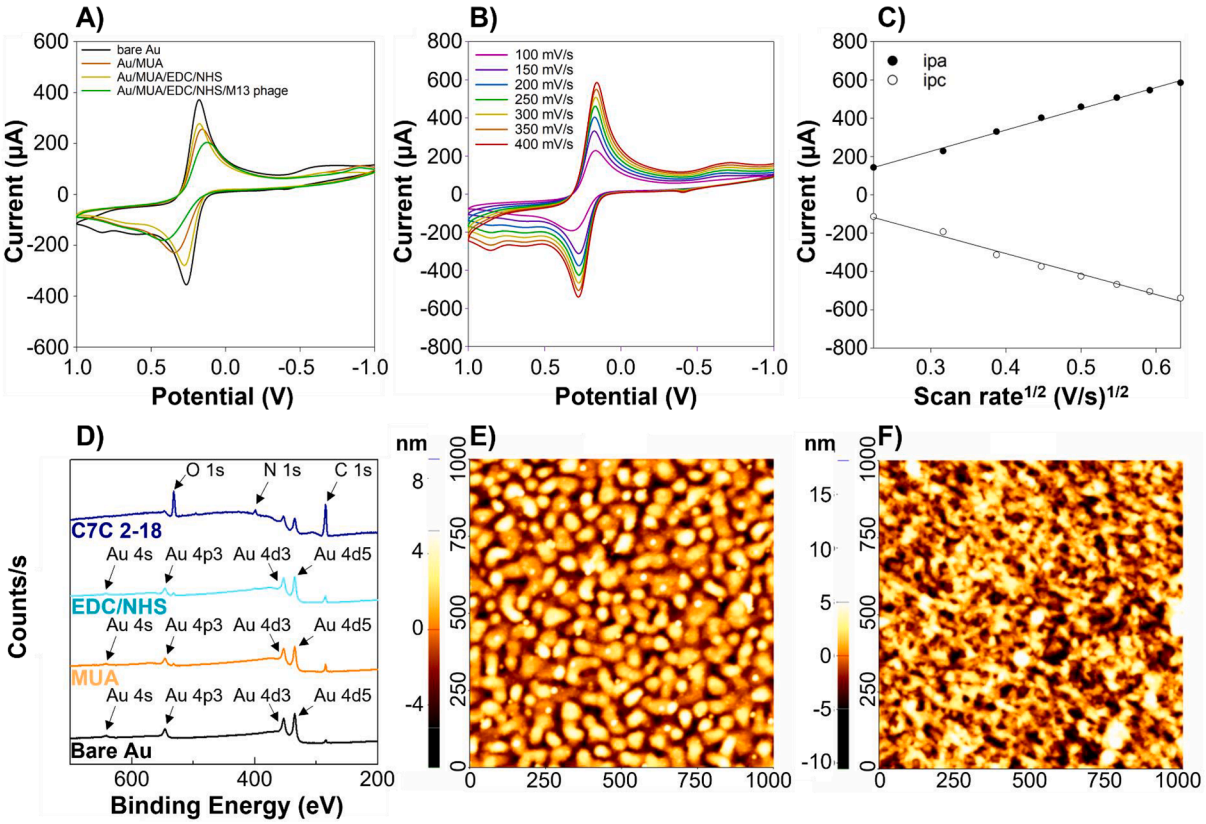

Fig. 2. Preparation of coupling chemistry (MUA-EDC/NHS) treated gold electrodes with whole phage particles. (A) Cyclic voltammograms of bare gold (black line), MUA treated gold surface (orange line), MUA-EDC/NHS treated gold surface (yellow line) and whole phage-tethered gold surface (green line). (B) Potential sweep rate dependance of redox peak current (i_{pa} and i_{pc}). (C) Atomic force micrograph of the whole phage-tethered gold surface. D) XPS survey spectrum. E) AFM image of bare gold, F) AMF image of C7C 2-18 phage on gold electrode.

slightly increased [15,26]. After that, chemical attachment of the whole M13 phage occurred on the gold electrode via covalent bonding through NHS ester, which can react with the amine group in the N-terminal domain of the p8 protein [26]. Further, to estimate the surface coverage of the M13 phage immobilized on the MUA-EDC/NHS-treated gold electrode, we used CV technique which is effective method to investigate whether and to what extension redox probes could adsorb on the surface of electrode [34]. The change in the peak currents with different scan rates was observed using CV (Fig. 2B). The anodic (i_{pa}) and cathodic (i_{pc}) peak current densities were proportional to the potential sweep rate (Fig. 2C), and the i_{pa}/i_{pc} ratio was close to unity (Fig. S2) [35]. In a controlled molecular diffusion process, the anodic to cathodic peak current ratio (i_{pa}/i_{pc}) is equal to 1 and remains constant with different scan rates. On the other hand, if redox species absorb on the surface of electrode, the values of i_{pa}/i_{pc} will differ from unity and vary with the scan rates due to the different behavior of the adsorbed oxidized and reduced forms [34,35]. According to these findings, as demonstrated in Fig. 2B, C and Fig. S2, we speculated electrochemical reactions of whole phage-tethered gold surface were fully controlled by molecular diffusion process.

3.2.2. Surface characterization of modified gold electrodes using AFM, SEM, and XPS

The covalent attachment of whole M13 phage particles was additionally confirmed by AFM, SEM and XPS analyses. XPS can provide intermolecular binding energy and the chemical structure of the modified gold surface. The XPS survey spectra of modified gold electrodes are shown in Fig. 2D. The changes in the elemental composition of carbon (C 1s), nitrogen (N 1s), oxygen (O 1s), and gold (Au 4d, Au 4p, and Au 4s) after each step were monitored. The bare gold spectrum showed peaks at 284, 334, 355, 532, 545, and 642 eV, which were assigned to C 1s, Au 4d5, Au 4d3, O 1s, Au 4p, and Au 4s, respectively. The weak peaks of the carbon and oxygen can be explained by the fact that the gold surface is able to absorb hydrocarbon contaminants from the atmosphere before XPS analysis. The functionalization of the gold electrode with MUA and activation of carboxylic acid (COOH) caused the peaks of carbon and oxygen to increase. After the EDC/NHS reaction, the COOH groups in MUA were converted into NHS ester groups ($C_4H_5NO_3$). Therefore, the peaks of carbon, nitrogen, and oxygen marginally increased. After that, attachment of phage particles (C7C 2-18) resulted in the relative elemental compositions of carbon, nitrogen, and oxygen on the surface due to the presence of amino acid residues of alanine, aspartic acid, and glutamic acid of M13 phage's major coat protein. Note that C7C 2-18 whole phage particles are covalently attached on the functionalized gold electrode through amide bonding (O═C—N), as expected (Fig. 2D).

We also performed AFM and SEM analyses to investigate the morphological changes between bare gold electrode and immobilization of phage on gold electrode. However, it was difficult to verify the fine changes because the surface roughness of the Au-coated wafer is large. Notwithstanding, no morphological changes on bare gold were observed (Figs. 2E and S3A). Unlikely, it was clearly seen that mass attachment of phage through either side-ways or zig-zag aligned bundling on the sensor layer (Figs. 2F and S3B). In the case of AFM, the histogram profile of the phage particles (C7C 2-18) bound to the gold electrode showed ~9 nm height differences, compared to those of bare electrode from the substrate surface (data not shown). In SEM measurements, the filamentous and twisted morphological changes of M13 phage on gold and silicon oxide substrate was confirmed as shown in Fig. S3C and D. The results suggested that successful immobilization of phage via MUA-EDC/NHS coupling chemistry, confirmed by XPS and mass deposition with nanofiber-like network structure on gold electrode, confirmed by AFM and SEM.

3.3. Validation of fabricated phage-based electrochemical biosensor

3.3.1. Effect of phage and protein concentration

To validate the electrochemical responses of a chemically modified whole phage sensor for the detection of caspase-3, the effects of phage and protein concentration were investigated by SWV measurements. The results showed that the value of current in SWV decreased with increasing phage concentration in the range of 10^8–10^{12} PFU/mL (Fig. S4A). This suggested that the number of caspase-3-specific peptides displayed on the surface of the phage increases their efficiency in binding caspase-3. A similar trend was observed with changes in caspase-3 protein concentration (Fig. S4B). We observed that the current in SWV gradually decreased with the increase in the amount of caspase-3.

3.3.2. Determination of sensor performance

We examined the performances of our developed phage sensor; the same concentration of the phage (~10^{12} PFU/mL) was immobilized on the gold surface using coupling chemistry (MUA-EDC/NHS) and further incubated with caspase-3 (0–1.2 μM). Then, the relative current changes were measured by SWV. After successful attachment of phages on the gold electrode, we tried to confirm the morphological changes between bare gold and functionalized phage sensor using atomic force microscopy (AFM). As clearly shown in Fig. 2E and F, filamentous fiber-like monolayer structure in C7C 2-18 phage functionalized gold electrode was seen, compared to the control, indicating chemically attachment of phage particles on gold electrode. In addition, we also observed that the binding affinity of the C7C 2-18 phage increased sequentially with an increase in caspase-3 concentration (Fig. 3A). Based on these investigations, we calculated the binding constant (K_d) of our developed sensor, which was found to be 0.13 ± 0.56 μM. In addition, the detection limit (LOD) of the whole phage sensor was calculated using the following equations [27]:

LOD = 3.3 × δ/s, where δ and s are the standard deviation of the regression line of the y-intercept and slope of the standard curve, respectively. As shown in Fig. 3B, the values of δ, s, and LOD for the whole phage sensor were 2.61, 22.11 ($y = 22.11x + 9.52$, $R^2 = 0.93$), and 0.39 μM, respectively.

3.3.3. Specificity of phage-based electrochemical biosensor

To test the specificity of the whole phage sensor, the change in ΔI % for different proteins (BSA, lysozyme, casein, thrombin, and caspase-9) was monitored using SWV measurements. As expected, our developed sensor showed specific binding to caspase-3, while low binding affinities were observed with other proteins such as BSA, lysozyme, casein, thrombin, and caspase-9 (Fig. 3C). In addition, it was clear seen that binding affinity of wild-type M13 was comparable to those of other proteins, indicating that successful screening of affinity peptides specific for caspase-3 via biopanning.

3.3.4. Reproducibility and stability of phage-based electrochemical biosensor

The reproducibility and stability are some of the most important factors in evaluating sensor performance in on-site detection. In our sensor, the reproducibility of the fabricated phage sensor was evaluated by determining the relative current change (ΔI %) with five different electrodes. The results clearly showed an acceptable relative standard deviation (RSD) of 4.67%, indicating remarkable reproducibility with good accuracy (Fig. S5). The stability of the three different fabricated phage sensors was monitored for 10 days. As shown in Fig. 3D, it was relatively stable up to 7 days. These results indicated that our developed phage sensor has remarkable stability for further field testing.

3.3.5. Detection of caspase-3 with hela cell lysates

Feasibility of the developed phage sensor for detection of caspase-3 activity was analyzed by SWV measurements with HeLa cell lysates, in

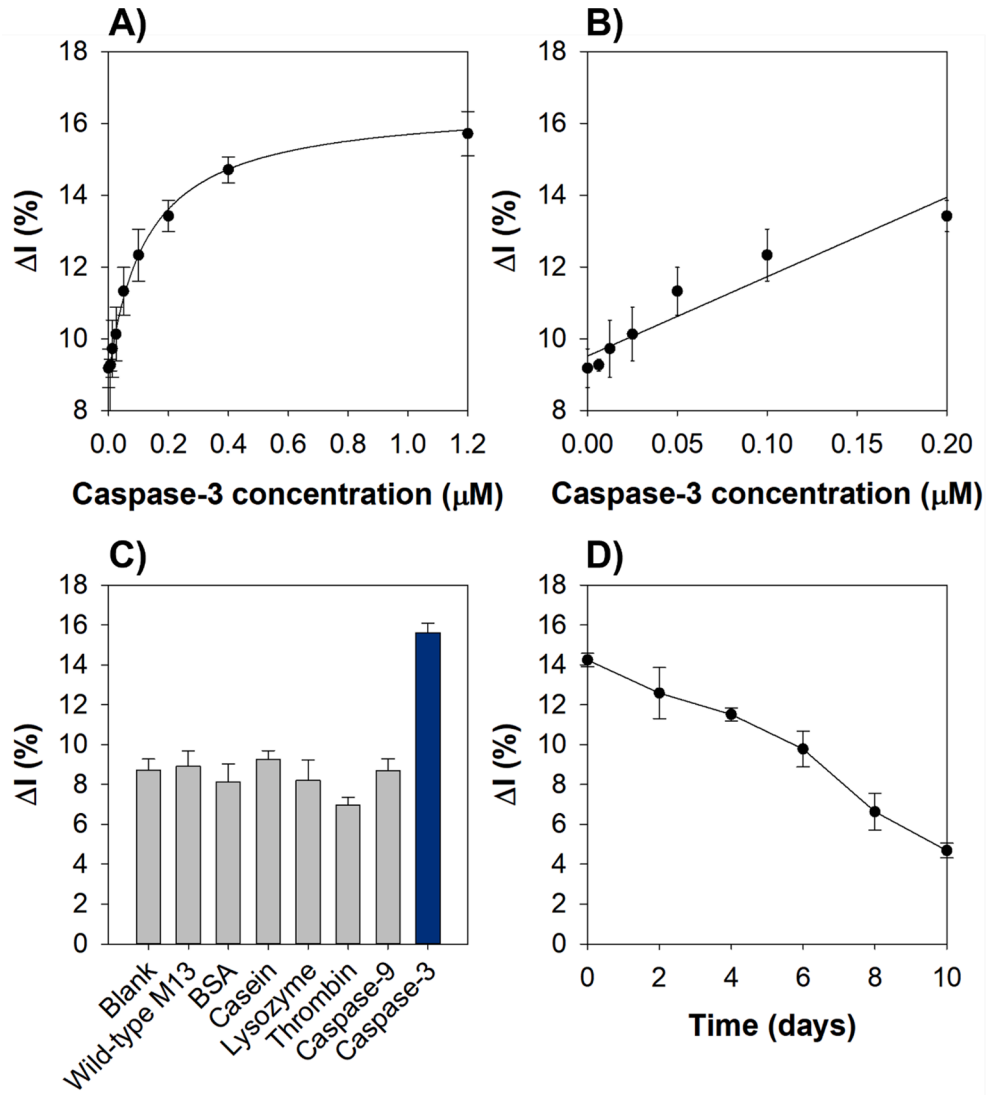

Fig. 3. Determination of performances of phage sensor. (A) Measurements of binding constant (K_d) of phage sensor for caspase-3. (B) The detection limit (LOD) of phage sensor on the MUA-EDC/NHS-functionalized gold chip. (C) Specificity test of the whole phage sensor. (D) Stability test of the whole phage sensor. All measurements were done in triplicate, and error bars represent standard deviations.

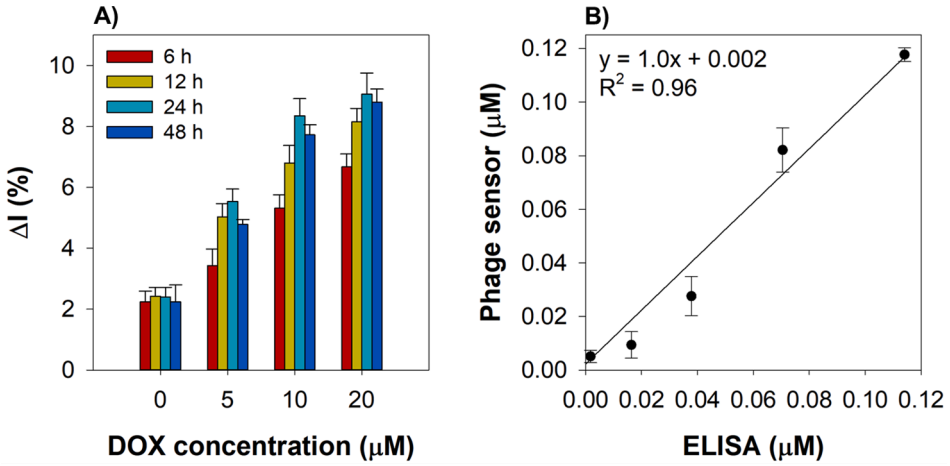

Fig. 4. The response of phage sensor for assay of caspase-3 activity with HeLa cell lysates. (A) Dynamic response of current change in HeLa cells treated with different concentration of DOX at different time-intervals. (B) Correlation between our developed phage sensor and commercially available ELISA for assay of caspase-3 activity with apoptotic HeLa cell lysates. All measurements were done in triplicate, and error bars represent standard deviations.

response to different doxorubicin (DOX) concentration. For this analysis, Hela cells were pre-treated with DOX at concentrations ranging from 0 to 20 μM and incubated at different time-intervals (0, 6, 12, 24, 48 h). The results showed that the value of current change (ΔI %) not only increased with the increase of DOX concentration but also with the longer-time of incubation of the cells. This is due to over-expression and activation of caspase-3 in the HeLa cells when treated DOX compared to the control. This is good agreement with previous study [5,28,29]. DOX can induce apoptosis in HeLa cells and have commonly used as apoptosis inducer against various cell lines. We also observed that the current change in all tested was correlated with the level of activated caspase-3 in apoptotic response (Fig. 4A). As expected, no significant changes were observed when wild-type M13 phages were incubated with DOX-induced HeLa cell lysates (Fig. S6).

Since caspase-3 plays an important role for understanding cell apoptosis along with different expression level derived from apoptosis chemical inducer, we performed the feasibility test of our developed phage sensor. As shown in Fig. S7, compared with HeLa cell lysates without both additions of DOX and known caspase-3 inhibitor (ZVADFMK, 100 μM), the relative current change increased remarkably, as our phage sensor was exposed to HeLa cell lysates pre-treated with DOX (20 μM) in the presence of known caspase-3 inhibitor. However, no significant change was observed when HeLa cells pretreated with the same concentration of DOX and caspase-3 inhibitor. This tendency is good agreement with previous reported [5]. However, our approach is no needing reagents or labels, a non-invasive operating process, the possibility of on-site analysis, and the use of simple instruments. From these observations, our developed phage sensor could only response in caspase-3 activation and detect caspase-3 activity in apoptotic HeLa cell lysates.

Applicability of biosensors is considered key parameters for evaluation of the possibility in a real testing or industrial commercialization. Therefore, additional experiments were performed with commercially available ELISA, to investigate applicability of the developed sensors, using SWV. As shown in Fig. 4B, the level of caspase-3, determined by our phage sensor were quite correlated with those of ELISA assay with good correlation coefficient (R^2) value of 0.96. In addition, in our developed phage sensor, the recovery (%) and RSD (%) values were found to be in the range of 98.2–104.4% and 3.9–5.7%. This result showed good recoveries of the phage sensor for detecting active caspase-3 in a complex biological sample (Table 2).

The comparison of assay performance for caspase-3 was summarized in Table 1. There are several studies for detection of caspase-3 with different detection regimes [30,31,32,33]. Compared to those obtained using different methods, our approach did not require complexed analytical equipment and enables fast response time for assay of caspase-3 activity with label-free and antibody-free.

Table 2
Analytical results of active caspase-3 detection in the presence of HeLa cell lysates.

Added concentration (nM)	Found concentration (nM)	Recovery (%)	RSD (%, n = 8)
12.5	12.3 ± 0.7	98.2 ± 5.6	5.7
25	26.1 ± 1.4	104.4 ± 5.4	5.2
50	50.5 ± 1.9	101.1 ± 3.9	3.9

4. Conclusions

In this study, we provide a novel approach to detect the cell apoptosis-related biomarker, caspase-3, with high sensitivity, selectivity, and reproducibility. We biopanned random peptide phage libraries (C7C) and identified the unique phage C7C 2-18 with the sequence CPTTMWRYC. This selected phage was used as an alternative recognition element for developing a whole phage-based electrochemical biosensor. Through chemical modification of the phage, whole phage particles were covalently attached to a gold surface. After that, a phage-based electrochemical biosensor was characterized for the detection of caspase-3. The developed phage-based electrochemical biosensor retained sufficient and significant electrochemical sensor performance. Under optimal conditions, the fabricated phage sensor showed a good binding affinity (K_d = 0.13 ± 0.56 μM) and limit of detection (0.39 μM) for caspase-3 detection. Furthermore, our developed phage sensor could be monitored the dynamic response of apoptotic HeLa cell induced by well-known apoptosis inducer, DOX. In summary, the developed electrochemical M13 phage sensor possesses several significant advantages over conventional methods. First, affinity peptide-displayed whole phage sensor can be easily applied onto functionalized electrodes and allows the simultaneous detection of caspase-3 with high specificity. Second, M13 phage used as receptor is harmless and can easily mass production and purification with a high yield at low cost. Third, rapid electrochemical response and relatively low sample volume (<20 μL) encourage the specialist to integrate for fabrication of micro total analytic systems or microdevices for a field test. Forth, our approach does not require sample labelling step to be analyzed and antibody. This sensing approach could serve as a viable means for evaluation of cell apoptosis by sensitive detection of caspase-3, and it could serve as an alternative to conventional receptors with high affinity and stability. Although our developed phage sensor exhibited satisfactory performances for caspase-3 assay, further work will be required for real testing. First, improvement of binding abilities in whole phage as molecular binder with chemical and/or genetic manipulation is challenging. Second, the use of phage-free peptides will be potential in the development of new caspase-3 assays for cancer diagnosis, as well as assaying in simultaneous monitoring of apoptotic cells grown in culture or artificially induced other cell lines.

CRediT authorship contribution statement

Jae Hwan Shin: Writing – original draft, Conceptualization, Methodology, Data curation. **Anam Rana Gul:** Data curation. **Moon Seop Hyun:** Data curation. **Chang-Hyung Choi:** Methodology, Data curation.

Table 1
Comparison of caspase-3 detection performances with the developed electrochemical phage sensor and other methods.

Detection method	Receptor/substrate	Binding constant	Detection limit	Operation to detection time	Reproducibility	Reference
Fluorometric and colorimetric biosensor	DEVD with AFC and pNA	ND	50 μM	ND	ND	[30]
Electrochemical biosensor	DEVD-HRP-signal amplifier	ND	100 pM	< 17 h	ND	[31]
Organic electrochemical sensor	Self-assembled monolayer with modified DEVD peptide with gold nanoparticle	ND	0.1 pM	< 49 h	ND	[32]
SERS-based biosensor	Magnetic-plasmonic nanopore	ND	50 pM	< 13.5 h	4.05–18.96%	[33]
M13 phage virus-based electrochemical sensor	Peptide-displayed M13 phage	0.13 ± 0.56 μM	0.39 μM	< 15 h	4.67%	This study

Abbreviations: ND, not determined; AFC, 7-amino-4-trifluoromethyl coumarin; pNA, p-nitroanilide; HRP, horseradish peroxidase; SERS, surface-enhanced Raman spectroscopy

Tae Jung Park: Conceptualization, Writing – review & editing. **Jong Pil Park:** Supervision, Conceptualization, Writing – review & editing, Funding acquisition.

Declaration of Competing Interest

The authors declare that they have no known competing financial interests or personal relationships that could have appeared to influence the work reported in this paper.

Acknowledgments

This work was supported by a National Research Foundation of Korea (NRF) grant funded by the Korean government (MSIT) (Nos. 2019R1A2C2084065 and 2021R1A4A1022206).

Appendix A. Supplementary material

Supplementary data to this article can be found online at https://doi.org/10.1016/j.bioelechem.2022.108090.

References

[1] X. Li, Y. Li, Q. Qiu, Q. Wen, Q. Zhang, W. Yang, L. Yuwen, L. Weng, L. Wang, Efficient biofunctionalization of MoS2 nanosheets with peptides as intracellular fluorescent biosensor for sensitive detection of caspase-3 activity, J. Colloid Interface Sci. 543 (2019) 96–105, https://doi.org/10.1016/j.jcis.2019.02.011.
[2] T.N.A. Pham, B. Le, S.H. Yang, Anticancer activity of the potential pyropia yezoensis galactan fractionated in human prostate cancer cells, Biotechnol. Bioprocess Eng. 26 (1) (2021) 63–70, https://doi.org/10.1007/s12257-020-0157-8.
[3] S. Shalini, L. Dorstyn, S. Dawar, S. Kumar, Old, new and emerging functions of caspases, Cell Death Differ. 22 (4) (2015) 526–539, https://doi.org/10.1038/cdd.2014.216.
[4] A.C. Clark, Caspase allostery and conformational selection, Chem. Rev. 116 (11) (2016) 6666–6706, https://doi.org/10.1021/acs.chemrev.5b00540.
[5] D. Deng, Y. Hao, S. Yang, Q. Han, L. Liu, Y. Xiang, F. Tu, N. Xia, A signal-on electrochemical biosensor for evaluation of caspase-3 activity and cell apoptosis by the generation of molecular electrocatalysts on graphene electrode surface for water oxidation, Sens. Actuat., B 286 (2019) 415–420, https://doi.org/10.1016/j.snb.2019.01.137.
[6] J. Yin, P. Miao, Apoptosis evaluation by electrochemical techniques, Chem. Asian J. 11 (5) (2016) 632–641, https://doi.org/10.1002/asia.201501045.
[7] N. Xia, Y. Huang, Z. Cui, S. Liu, D. Deng, L. Liu, J. Wang, Impedimetric biosensor for assay of caspase-3 activity and evaluation of cell apoptosis using self-assembled biotin-phenylalanine network as signal enhancer, Sens. Actuat., B 320 (2020) 128436, https://doi.org/10.1016/j.snb.2020.128436.
[8] Y. Pan, M. Guo, Z. Nie, Y. Huang, Y. Peng, A. Liu, M. Qing, S. Yao, Colorimetric detection of apoptosis based on caspase-3 activity assay using unmodified gold nanoparticles, Chem. Commun. 48 (7) (2012) 997–999, https://doi.org/10.1039/C1CC15407A.
[9] Q. Wang, W. Hu, Q. Feng, X.-H. Cao, W. Chai, C. Yi, M.-J. Li, Coumarin-modified gold nanoprobes for the sensitive detection of caspase-3, RSC Adv. 5 (54) (2015) 43824–43830, https://doi.org/10.1039/C5RA05350A.
[10] H. Shi, R.T.K. Kwok, J. Liu, B. Xing, B.Z. Tang, B. Liu, Real-time monitoring of cell apoptosis and drug screening using fluorescent light-up probe with aggregation-induced emission characteristics, J. Am. Chem. Soc. 134 (43) (2012) 17972–17981, https://doi.org/10.1021/ja3064588.
[11] Y. Yuan, C.-J. Zhang, R.T.K. Kwok, D. Mao, B.Z. Tang, B. Liu, Light-up probe based on AIEgens: dual signal turn-on for caspase cascade activation monitoring, Chem. Sci. 8 (4) (2017) 2723–2728, https://doi.org/10.1039/C6SC04322D.
[12] T. Kihara, C. Nakamura, M. Suzuki, S.-W. Han, K. Fukazawa, K. Ishihara, J. Miyake, Development of a method to evaluate caspase-3 activity in a single cell using a nanoneedle and a fluorescent probe, Biosens. Bioelectron. 25 (1) (2009) 22–27, https://doi.org/10.1016/j.bios.2009.05.036.
[13] S. Wen, Y. Su, R. Wu, S. Zhou, Q. Min, G.-C. Fan, L.-P. Jiang, R.-B. Song, J.-J. Zhu, Plasmonic Au nanostar raman probes coupling with highly ordered TiO2/Au nanotube arrays as the reliable SERS sensing platform for chronic myeloid leukemia drug evaluation, Biosens. Bioelectron. 117 (2018) 260–266, https://doi.org/10.1016/j.bios.2018.06.001.
[14] H. Chen, Q. Mei, Y. Hou, X. Zhu, K. Koh, X. Li, G. Li, Fabrication of a protease sensor for caspase-3 activity detection based on surface plasmon resonance, Analyst 138 (2013) 5757–5761, https://doi.org/10.1039/C3AN01137B.
[15] H. Chen, J. Zhang, Y. Gao, S. Liu, K. Koh, X. Zhu, Y. Yin, Sensitive cell apoptosis assay based on caspase-3 activity detection with graphene oxide-assisted electrochemical signal amplification, Biosens. Bioelectron. 68 (2015) 777–782, https://doi.org/10.1016/j.bios.2015.02.007.
[16] S. Song, X. Shang, J. Zhao, X. Hu, K. Koh, K. Wang, H. Chen, Sensitive and selective determination of caspase-3 based on calixarene functionalized reduction of graphene oxide assisted signal amplification, Sens. Actuat., B 267 (2018) 357–365, https://doi.org/10.1016/j.snb.2018.03.185.
[17] Y. Wang, V. Selvamani, I.-K. Yoo, T.W. Kim, S.H. Hong, A novel strategy for the microbial removal of heavy metals: cell-surface display peptides, Biotechnol. Bioprocess Eng. 26 (2021) 1–9, https://doi.org/10.1007/s12257-020-0218-z.
[18] S.W. Cho, H.J. Ko, T.H. Park, Identification of a lung cancer biomarker using a cancer cell line and screening of olfactory receptors for biomarker detection, Biotechnol. Bioprocess Eng. 26 (1) (2021) 55–62, https://doi.org/10.1007/s12257-020-0132-4.
[19] T.-Y. Kim, J.W. Lim, M.-C. Lim, N.-E. Song, M.-A. Woo, Aptamer-based fluorescent assay for simple and sensitive detection of fipronil in liquid eggs, Biotechnol. Bioprocess Eng. 25 (2) (2020) 246–254, https://doi.org/10.1007/s12257-019-0358-1.
[20] S.H. Lim, Y.C. Ryu, B.H. Hwang, Aptamer-immobilized gold nanoparticles enable facile and on-site detection of staphylococcus aureus, Biotechnol. Bioprocess Eng. 26 (1) (2021) 107–113, https://doi.org/10.1007/s12257-020-0161-z.
[21] S.M. Lee, S. Shin, H.Y. Kim, B.Y. Won, J.K. Ahn, K.S. Park, H.G. Park, Washing-free electrochemical strategy to detect target DNA utilizing peroxidase mimicking DNAzyme, Biotechnol. Bioprocess Eng. 25 (5) (2020) 707–714, https://doi.org/10.1007/s12257-020-0272-6.
[22] S. Mittal, H. Kaur, N. Gautam, A.K. Mantha, Biosensors for breast cancer diagnosis: a review of bioreceptors, biotransducers and signal amplification strategies, Biosens. Bioelectron. 88 (2017) 217–231, https://doi.org/10.1016/j.bios.2016.08.028.
[23] C. Mao, A. Liu, B. Cao, Virus-based chemical and biological sensing, Angew. Chem. Int. Ed. 48 (37) (2009) 6790–6810, https://doi.org/10.1002/anie.200900231.
[24] J.-S. Moon, E.J. Choi, N.-N. Jeong, J.-R. Sohn, D.-W. Han, J.-W. Oh, Research progress of M13 bacteriophage-based biosensors, Nanomaterials 9 (2019) 1448, https://doi.org/10.3390/nano9101448.
[25] J. Paczesny, K. Bielec, Application of bacteriophages in nanotechnology, Nanomaterials 10 (10) (2020) 1944, https://doi.org/10.3390/nano10101944.
[26] T.-C. Tsai, C.-W. Liu, Y.-C. Wu, N.A.P. Ondevilla, M. Osawa, H.-C. Chang, In situ study of EDC/NHS immobilization on gold surface based on attenuated total reflection surface-enhanced infrared absorption spectroscopy (ATR-SEIRAS), Colloids Surf., B 175 (2019) 300–305, https://doi.org/10.1016/j.colsurfb.2018.12.009.
[27] J.H. Kim, C.H. Cho, J.H. Shin, M.S. Hyun, E. Hwang, T.J. Park, J.P. Park, Biomimetic isolation of affinity peptides for electrochemical detection of influenza virus antigen, Sens. Actuat., B 343 (2021) 130161, https://doi.org/10.1016/j.snb.2021.130161.
[28] Y. Yuan, C.J. Zhang, R.T.K. Kwok, D. Mao, B. Liu, Light-up probe based on AIEgens: dual signal turn-on for caspase cascade activation monitoring, Chem. Sci. 8 (2017) 2723–2728, https://doi.org/10.1039/c6sc04322d.
[29] C.-S. Bae, C.-M. Lee, T. Ahn, Encapsulation of apoptotic proteins in lipid nanoparticles to induce death of cancer cells, Biotechnol. Bioprocess Eng. 25 (2) (2020) 264–271, https://doi.org/10.1007/s12257-019-0409-7.
[30] V. Gurtu, S.R. Kain, G. Zhang, Fluorometric and colorimetric detection of caspase activity associated with apoptosis, Anal. Biochem. 251 (1) (1997) 98–102, https://doi.org/10.1006/abio.1997.2220.
[31] B. Khalilzadeh, N. Shadjou, M. Eskandani, H.N. Charoudeh, Y. Omidi, M.-R. Rashidi, A reliable self-assembled peptide based electrochemical biosensor for detection of caspase 3 activity and apoptosis, RSC Adv. 5 (72) (2015) 58316–58326, https://doi.org/10.1039/C5RA08561F.
[32] J.i. Yu, A. Yang, N. Wang, H. Ling, J. Song, X.i. Chen, Y. Lian, Z. Zhang, F. Yan, M. Gu, Highly sensitive detection of caspase-3 activity based on peptide-modified organic electrochemical transistor biosensors, Nanoscale 13 (5) (2021) 2868–2874, https://doi.org/10.1039/D0NR08453K.
[33] G. Qi, D. Sun, Y.u. Tian, C. Xu, Y. Zhang, D. Wang, K. Ma, S. Xu, Y. Jin, Fast activation and tracing of caspase-3 involved cell apoptosis by combined electrostimulation and smart signal-amplified SERS nanoprobes, Anal. Chem. 92 (11) (2020) 7861–7868, https://doi.org/10.1021/acs.analchem.0c0111410.1021/acs.analchem.0c01114.s001.
[34] J.C. Zuaznabar-Gardona, A. Fragoso, Electrochemical characterisation of the adsorption of ferrocenemethanol on carbon nano-onion modified electrodes, J. Electroanal. Chem. 871 (2020) 114314, https://doi.org/10.1016/j.jelechem.2020.114314.
[35] T. Matsubara, M. Ujie, T. Yamamoto, M. Akahori, Y. Einaga, T. Sato, Highly sensitive detection of influenza virus by boron-doped diamond electrode terminated with sialic acid-mimic peptide, Proc. Natl. Acad. Sci. 113 (32) (2016) 8981–8984, https://doi.org/10.1073/pnas.1603609113.